THE JOURNAL OF PHYSICAL CHEMISTRY B

ARTICLE

pubs.acs.org/JPCB

Molecular Dynamics Simulation Study of Glycerol−Water Liquid Mixtures

Andrei V. Egorov,[†] Alexander P. Lyubartsev,[‡] and Aatto Laaksonen[*,‡]

[†]Faculty of Physics, St. Petersburg University, St. Petersburg 198504, Russia

[‡]Department of Materials and Environmental Chemistry, Division of Physical Chemistry, Arrhenius Laboratory, Stockholm University, Stockholm 106 91, Sweden

ABSTRACT: To study the effects of water on conformational dynamics of polyalcohols, Molecular Dynamics simulations of glycerol−water liquid mixtures have been carried out at different concentrations: 42.9 and 60.0 wt % of glycerol, respectively. On the basis of the analysis of backbone conformer distributions, it is found that the surrounding water molecules have a large impact on the populations of the glycerol conformers. While the local structure of water in the liquid mixture is surprisingly close to that in pure liquid water, the behavior of glycerols can be divided into three different categories where roughly 25% of them occur in a structure similar to that in pure liquid of glycerol, ca. 25% of them exist as monomers, solvated by water, and the remaining 50% of glycerols in the mixture form H-bonded strings as remains of the glycerol H-bond network. The typical glycerol H-bond network still exists even at the lower concentration of 40 wt % of glycerol. The microheterogeneity of water−glycerol mixtures is analyzed using time-averaged distributions of the sizes of the water aggregates. At 40 wt % of glycerol, the cluster sizes from 3 to 10 water molecules are observed. The increase of glycerol content causes a depletion of clusters leading to smaller 3−5 molecule clusters domination. Translational diffusion coefficients have been calculated to study the dynamical behavior of both glycerol and water molecules. Rotational-reorientational motion is studied both in overall and in selected substructures on the basis of time correlation functions. Characteristic time scales for different motional modes are deduced on the basis of the calculated correlation times. The general conclusion is that the presence of water increases the overall mobility of glycerol, while glycerol slows the mobility of water.

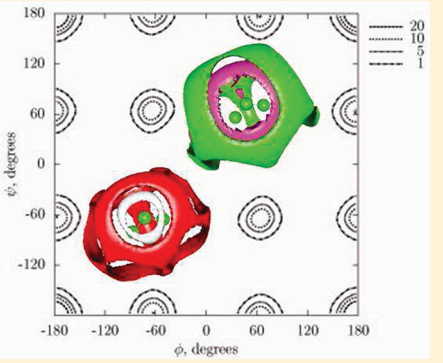

1. INTRODUCTION

Glycerol (propane-1,2,3-triol) is a sweet-tasting, highly viscous three-carbon sugar alcohol with three hydroxyl groups. It is highly flexible, containing only single bonds, allowing large and highly complex structural fluctuations, complicated conformational behavior, and a rich intra- and intermolecular hydrogen-bond network. Its high flexibility makes it also a good glass-former, and it can be supercooled to −86 °C ($T_{melting}$ = 18 °C and $T_{boiling}$ = 290 °C). It is completely soluble in water and many alcohols but not in hydrocarbons. Glycerol is a part of the backbone in fats and phospholipids. Glycerol is important in many industrial areas including cosmetics and drugs as well as food. It is also the main substance to produce nitro glycerine, a basic ingredient in dynamite, and a common pain reliever for heart-disorder patients. Glycerol is also among the best cryo-protectant solvents to preserve proteins.[1]

In aqueous solutions, glycerol is suggested to disrupt the hydrogen-bonded structure of water, thereby making the solution more compact.[2] Surface composition of glycerol−water mixtures is found to deviate from that in the bulk so that the surface is enriched with glycerol, while the vapor above the solution is almost 100% water.[3] In dielectric spectroscopy studies, Puzenko et al. found a critical mole fraction X, where the glycerol hydrogen bonds are in balance with water hydrogen bonds: $X = 100\%n_w/(n_w + n_g) = 40$ mol %, because glycerol can be involved with roughly 6 (n_g) hydrogen bonds, while water molecules can form 4 (n_w).[4,5] Glycerol can stabilize the structure of biomolecules. In their theoretical work, Shulgin and Ruckenstein found water in excess in the vicinity of ribonuclease A when it was solvated in water−glycerol mixture, preserving the protein. If the same protein was dissolved in a water−urea mixture, it was found that urea came closest to the protein potentially leading to denaturation of the protein.[6] In general, adding more glycerol stabilizes proteins in aqueous solutions,[7] affecting their folding.[8] Chen et al. report how the Stokes−Einstein relation (giving a diffusion coefficient proportional to temperature divided by viscosity) breaks down for supercooled aqueous solutions of glycerol, but becomes valid with increasing water concentration.[9]

To gain insight and to better understand the intriguing properties of water−glycerol mixtures, atomistic Molecular Dynamics (MD) simulations are useful. Many studies can be found in the literature from the last two decades of which we quickly review a few here below. The first MD simulation of pure glycerol was carried out by Root and Stillinger,[10] who studied the

Received: July 10, 2011
Published: October 17, 2011

Table 1. Simulated Systems

	system			
	I	II	III	IV
no. of water molecules	340	340	0	256
no. of glycerol molecules	50	100	256	0
glycerol conc., weight percent	42.9	60.0	100.0	0.0
equilibration time, ns	3.0	3.0	2.0	0.4
simulation time, ns	10.0	5.0	5.0	1.0
calc. density, g cm^{-3}	1.103	1.144	1.223	0.995
expt density,[a] g cm^{-3}	1.106	1.149	1.261	0.997
calc. $D_{glycerol}$, $\times 10^9$ m^2 s^{-1}	0.26	0.11	0.01	
calc. D_{water}, $\times 10^9$ m^2 s^{-1}	0.97	0.52		2.47

[a] Data from ref 32.

short-range order in the ambient and supercooled liquids. They constructed a nine-site model for glycerol where both CH and CH_2 groups were treated as "united atoms". They later used the same potential in the simulation of the resorufin sodium salt in low-temperature glycerol glass[11] and in the modeling of the pressure effect on hydrogen bonding in glycerol.[12] Benjamin et al. developed another nine-site potential for glycerol to simulate the scattering of Ne and water from liquid glycerol surfaces[13] as well as collisions of an HCl molecule with the glycerol surface.[14] Padro and co-workers[15,16] have performed a series of MD simulations of H-bonded liquids including glycerol using the OPLS parameter set proposed by Jorgensen and co-workers[17] for alcohols. Their study focuses mainly on the hydrogen-bonding statistics. Chelli and co-workers[18−21] adopted the AMBER force field to develop the very first all-atom model for glycerol, which they then used to perform a fairly extensive series of classical MD simulation studies of glycerol over a wide range of temperatures to investigate the internal dynamics, conformational distribution, and hydrogen bonding. In general, a good agreement with experimental structural and thermodynamical data was achieved, except that the calculated diffusion coefficients did differ from the experimental ones quite considerably. Blieck et al.[22] reparameterized the potential model proposed by Chelli et al. and succeeded in reproducing the glycerol diffusion coefficient much better. Callam et al. report a comprehensive ab initio analysis of potential energy surfaces of glycerol.[23] Zhuang and Dellago[24] carried out a 21.5 ps CPMD simulation of 16 glycerol molecules in a periodic box at the experimental density, but due to the very short simulation, their results on transport properties provide only rather rough estimates. Dashnau et al.[25] performed MD and IR studies of hydrogen-bond patterns of glycerol and its mixtures with water using the all-atoms CHARMM22 force field[26] for glycerol and the TIP3P water model. Yongye et al.[27] focused on examining the rotational isomeric states of glycerol at infinitely dilute aqueous solution via 1 μs MD and 40 ns Replica Exchange MD simulations using the TIP3P water model. Chen et al.[28,29] performed a detailed MD study of hydrogen bonding in glycerol aqueous solutions utilizing CHARMM22 force field[26] for glycerol and the SPC/E water model. Kyrychenko and Dyubko[30] who investigated the mixing of glycerol slab with the bulk water at 323 K via MD simulations found that mixing may be described as taking place via two regimes, fast and slow. The time of fast initial mixing stage was estimated to 5 ns for glycerol−water and 3.5 ns for glycerol−glycerol partners.

Table 2. Bond, Angle, and Torsional Parameters of the Glycerol Force Field

	$V_{bonds} = K_b(r - r_0)^2$					
	K_b, kcal mol^{-1} $Å^{-2}$			r_0, Å		
bond	refs 18,22	ref 26	ref 34	refs 18,22	ref 26	ref 34
CC	**310.0**	222.5	255.0	**1.526**	1.516	1.509
CO	**320.0**	428.0	360.0	**1.410**	1.420	1.410
CH	rigid bond	**309.0**	335.0	**1.090**	1.111	1.093
OH	rigid bond	**545.0**	535.0	**0.960**	0.960	0.955

	$V_{angles} = K_\theta(\theta - \theta_0)^2$			
	K_θ, kcal mol^{-1} rad^{-2}		θ_0, deg	
angle	refs 18,22	ref 26	refs 18,22	ref 26
CCC	**40.0**	53.35	**109.5**	111.0
CCO	**50.0**	75.7	**109.5**	110.1
CCH	**50.0**	34.5	**109.5**	110.1
COH	**55.0**	57.5	**108.5**	106.0
HCH	**35.0**	35.5	**109.5**	109.0
OCH	**50.0**	45.9	**109.5**	108.89

	$V_{torsions} = K_\phi(1 + \cos(n\phi))$			
	K_ϕ, kcal mol^{-1}		n	
torsion type	refs 18,22	ref 26	refs 18,22	ref 26
CCCH	**0.1556**	0.15	**3**	3
CCCO	**0.1556**	0.15	**3**	3
CCCO		0.68		1
OCCO	**0.1440**	0.30	**3**	3
OCCO	**1.0000**	−1.93	**2**	1
OCCH	**0.1556**	0.15	**3**	3
HOCC	**0.1667**	0.140	**3**	3
HOCH	**0.1667**	0.140	**3**	3
HCCH	**0.1556**	0.15	**3**	3

The slow component was extrapolated to 1−5 μs. Recently, Busselez et al.[31] carried out the MD simulations of liquid glycerol confined in the cylindrical silica nanopore using the AMBER force field reparameterized by Blieck et al.[22]

Despite numerous computational studies on glycerol, several phenomena such as the microheterogeneity, formation of water/glycerol microaggregates (domains), distribution of their sizes, etc., are still poorly understood. In the present study, two glycerol−water mixtures with 42.9 and 60.0 wt % of glycerol, respectively, are studied by MD simulations. Also, pure glycerol and water were simulated as the reference systems. The characteristic data on the studied systems are collected in Table 1.

At concentrations up to 30 wt % of glycerol, the water content is higher than 10 molecules per 1 glycerol, and solute molecules are mainly monomerically dispersed and surrounded by the solvent. This fact can be illustrated with glycerol carbon−carbon RDF published by Chen et al. (see Figure 1A from ref 29) where a single weak maximum was observed at about 5.5 Å. In the 42 and 60 wt % region, respectively, the water content is 7.0 and 3.4 molecules per glycerol, and a depletion of bulk water pool is observed. At higher (≥75 wt %) glycerol concentrations, water content is

dx.doi.org/10.1021/jp208758r |J. Phys. Chem. B 2011, 115, 14572–14581

Table 3. Lennard-Jones Parameters and Atomic Charges of the Glycerol Force Field

$$V_{\text{Lennard-Jones}} = 4\sqrt{\varepsilon_i \varepsilon_j}\left(\left(\frac{\sigma_i + \sigma_j}{2R_{ij}}\right)^{12} - \left(\frac{\sigma_i + \sigma_j}{2R_{ij}}\right)^{6}\right)$$

	σ, Å			ε, kcal mol^{-1}		
atom	ref 18	ref 22	ref 26	ref 18	ref 22	ref 26
C	3.816	**3.816**	4.054	0.1094	**0.1094**	0.020
O	3.442	**2.8508**	3.029	0.2100	**0.1591**	0.1521
aliphatic H	2.774	**2.774**	2.352	0.0157	**0.0157**	0.022
hydroxyl H	0	**1.4254**	0.400	0	**0.0498**	0.046

$$V_{\text{Coulomb}} = \frac{q_i q_j e^2}{R_{ij}}$$

	q, electronic units		
atom	ref 18	ref 22	ref 26
terminal C	0.182	**0.182**	0.05
central C	0.055	**0.055**	0.14
terminal aliphatic H	0.026	**0.026**	0.09
central aliphatic H	0.040	0.026[a]	0.09
hydroxyl H	0.396	**0.4158**	0.43
terminal O	−0.585	**-0.6048**	−0.66
central O	−0.581	**-0.6048**	−0.66

[a] In the present study, the atomic charge of the central aliphatic hydrogen was increased to **0.044** electronic units to bring the net glycerol molecule charge to zero.

lower than 2 molecules per glycerol, and water presumably loses its hydrogen-bond network and mixes into the solution as a composition of isolated molecules and/or water pairs.

2. METHODS

2.1. Interaction Potentials for Glycerol. To date, four all-atom force fields for glycerol have been proposed: the AMBER force field as adopted by Chelli et al.,[18] its reparameterized version by Blieck et al.,[22] and two variants of the CHARMM force-field proposed by Reiling et al.[26] and that by Hatcher et al.[33] The variant of Reiling et al. has not yet been tested much against the experimental data concerning the structure and dynamics of glycerol. The simulations using the force field parametrized by Hatcher et al.[33] have given diffusion coefficients for binary water−alditols solutions systematically almost −50% lower than the experimental ones. The potential model proposed by Blieck et al.[22] reproduces the features of liquid glycerol best among the AMBER-based force fields. However, in this force field, the glycerol molecule is not treated as fully flexible. The bonds involving hydrogen atoms are kept rigid, which may affect hydrogen-bonding properties.

In our simulations, a slightly modified version of Blieck et al. force-field for glycerol is used. The summary of the glycerol potential parameters used in our and in some other works is presented in Tables 2 and 3. As compared to the original paper,[22] the atomic charge of the central aliphatic hydrogen was increased to 0.044 electronic units to bring the net glycerol molecule charge to zero (not the case in the original parametrization). The stretching type potentials for C−H and

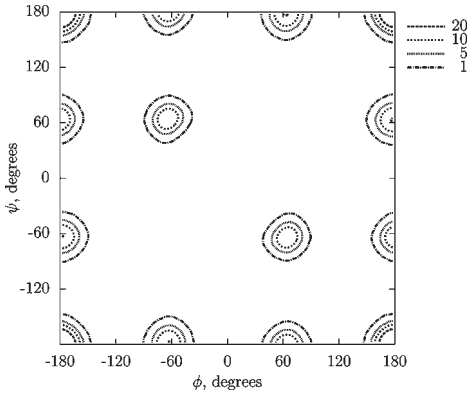

Figure 1. Ramachandran plot of the permitted values of two C−C−C−$O_{terminal}$ torsion angles ϕ and ψ. System **I**.

O−H bonds were added also. The bond force constants were taken from the CHARMM22 force field,[26] which are based on high-level ab initio calculations. Moreover, these values are quite close to the ones proposed by Mellberg and Rasmussen,[34] and later employed by Root and Stillinger in their glycerol simulations.[10,11] The parameters used in the present simulations are displayed in Tables 2 and 3 by the bold font. The flexible SPC-F water potential by Toukan and Rahman[35] was chosen for this study because it has been previously shown[36] to reproduce the structure and dynamics of water reasonably well. The potential energy function (force field), V_{total}, is defined as a sum of the following five terms:

$$V_{\text{total}} = V_{\text{bonds}} + V_{\text{angles}} + V_{\text{torsions}} + V_{\text{Lennard-Jones}} + V_{\text{Coulomb}}$$

2.2. Computational Details. MDynaMix[37] package was used in the present simulations. All simulations were carried out in an isothermal−isobaric (NPT) ensemble in a cubic periodic cell at 25 °C and atmospheric pressure. Temperature was kept constant by using the Nosé−Hoover method,[38,39] and the pressure was regulated by the Hoover barostat.[40] The equations of motion were solved using the double time step algorithm by Tuckerman et al.[40,41] with a long time step equal to 10 short time steps of 0.2 fs. The long-range Coulomb forces were calculated using the Ewald summation method. The length of simulations is given in Table 1 together with other characteristic data from the simulations.

3. RESULTS AND DISCUSSION

3.1. Conformational States and Distributions. The traditional classification of glycerol conformational isomers, proposed by Bastiansen,[42] is based on the concept of six backbone conformers. According to this concept, the relative position of each terminal CH_2OH group with respect to the rest of carbon and oxygen atoms may be characterized by three possible conformations labeled as α, β, and γ. In the α conformation, the terminal oxygen atom is in trans position to the opposite terminal carbon; in the β conformation, the oxygens of the terminal CH_2OH and central CHOH groups are in trans positions; and in the γ conformation, the oxygen atom of the terminal group is in trans position with respect to the aliphatic hydrogen atom of the central CHOH group. In total, six backbone conformers, $\alpha\alpha$, $\alpha\beta$, $\alpha\gamma$, $\beta\beta$, $\beta\gamma$, and $\gamma\gamma$, are possible.

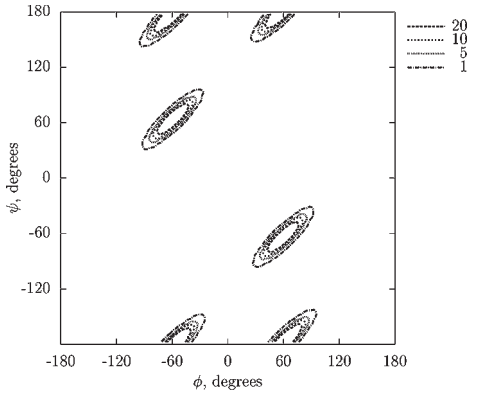

Figure 2. Ramachandran plot of the permitted values of the torsion angles $O_{terminal}-C-C-O_{central}$, ϕ, and $C-C-C-O_{terminal}$, ψ. System **I**.

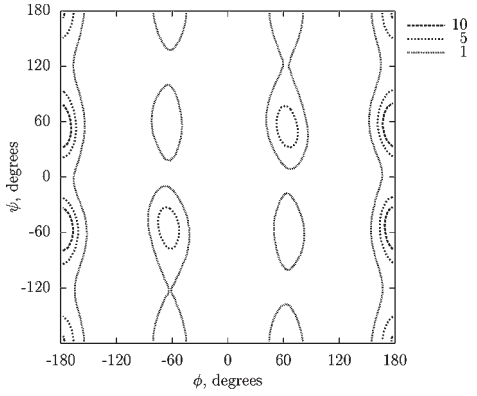

Figure 3. Ramachandran plot of the permitted values of the torsion angles $C-C-C-O_{terminal}$, ϕ, and $H_{terminal}-O_{terminal}-C-C$, ψ. System **I**.

However, all of these conformations are specified irrespective of the positions of the hydroxyl group hydrogens. We describe the all-atom conformational space of glycerol using combinations of six torsion angles: two $C-C-C-O_{terminal}$, one $O_{terminal}-C-C-O_{central}$, and three $H-O-C-C$ about each $C-O$ bond. A detailed view on the conformational distributions can be given using two-dimensional maps or Ramachandran plots,[43,44] indicating the most probable combinations of neighboring torsion angles. Five Ramachandran plots for glycerol calculated for 42.9 wt % mixture (system **I**) are shown in Figures 1−5. The corresponding Ramachandran plots for the other systems are similar and are therefore not displayed.

Yongye et al.,[27] who carried out the 1 μs MD simulation of glycerol to study its isomeric states at infinitely dilute aqueous solution, performed a long 150 ns equilibration to ensure reliable rotamer distributions. In the present work, we have a high concentration of glycerols ensuring a proper enough sampling of the conformational space in a much shorter simulation (see Table 1) than reported in ref 27.

The conformational distributions of glycerol backbone in various glycerol−water mixtures are collected in Table 4 and compared to the available data from literature. The $\alpha\alpha$ structure is found as the most abundant in all simulated glycerol−water mixtures. The $\beta\beta$ and $\gamma\gamma$ conformers give only a negligible contribution. All other forms, $\alpha\beta$, $\alpha\gamma$, and $\beta\gamma$, contribute about 60% in total. Our results on pure glycerol

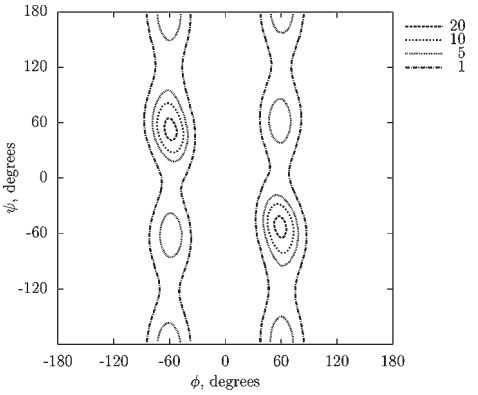

Figure 4. Ramachandran plot of the permitted values of the torsion angles $O_{terminal}-C-C-O_{central}$, ϕ, and $H_{terminal}-O_{terminal}-C-C$, ψ. System **I**.

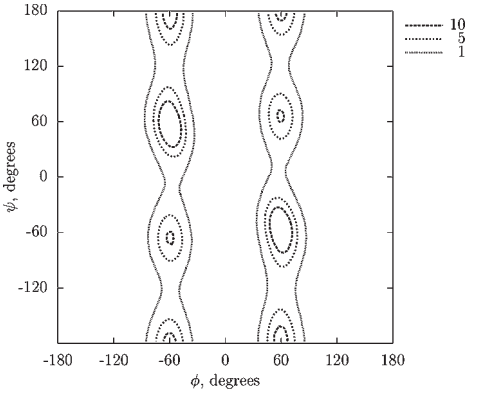

Figure 5. Ramachandran plot of the permitted values of the torsion angles $O_{terminal}-C-C-O_{central}$, ϕ, and $H_{central}-O_{central}-C-C$, ψ. System **I**.

rotamer populations deviate from both earlier MD results, those of Chelli et al.[19] and those of Chen et al.,[29] as well as from neutron diffraction data of Towey et al.[46] The rotamer populations appear to be very sensitive to the force field model used, which is different in these works. Also, they converge slowly and thereby depend on the length of the simulation to allow a proper sampling. Concerning the corresponding results for the water−glycerol mixtures, our results are consistent with several earlier investigations: ab initio calculations,[23] ^{1}H NMR experiments,[23,45] and MD studies by Dashnau et al.[25] as well as those by Yongye et al.[27] However, they differ from the MD results of Chen et al.[29] In general, there is a good agreement between the experimental[23,45] and calculated[23,27] rotamer populations for water-rich mixtures among the previous investigations concerning the conformational states.

The rotamer populations in pure glycerol and its water solution differ from each other. The main effect of the water when added into glycerol is its capability to disrupt the hydrogen bonds within the glycerol network, thereby allowing the rotamer populations to change more freely due to intermolecular interactions. According to the MD simulation results of Dashnau et al.[25] and Chen et al.,[29] the conformational distributions depend only slightly on the glycerol concentration. In our simulations, see Table 4, the presence of water molecules leads

Table 4. Glycerol Backbone Conformations Probability Distributions in Water−Glycerol Mixtures in Percent

		conformer						
method	glycerol conc., wt %	$\alpha\alpha$	$\alpha\beta$+$\beta\alpha$	$\alpha\gamma$+$\gamma\alpha$	$\beta\gamma$+$\gamma\beta$	$\gamma\gamma$	$\beta\beta$	ref
MD	42.9	37.1	22.0	22.6	18.0	0.16	0.06	this study
	60.0	37.2	20.8	27.2	14.4	0.22	0.06	
	100.0	39.5	24.6	25.8	9.8	0.11	0.14	
MD	100.0	48 ± 1	1.4 ± 0.4	46.0 ± 0.6	0.2 ± 0.1	4.4 ± 0.6	0	19
^{1}H NMR	5	14−25	13−25	25−35	13−18	6−18	3−8	45
SM5.42/HF and DFT		18−30	20−23	27−28	16−24	4	2−3	23
^{1}H NMR	5	18−20	20−22	28−30	15	10−12	5	
MD	n/a	40	20	30	5	5	0	25
MD	13.9	79.7	10.2	9.6	0.43	0.02	0.05	28,29
	21.1	83.5	8.7	7.5	0.06	0.07	0.15	
	29.7	79.7	9	10	0.89	0	0.015	
	34.0	81	10.7	7.9	0.21	0.06	0.18	
	39.3	79.7	9	10	0.89	0	0.02	
	44.0	78	8.6	12.6	0.76	0.07	0.02	
	100.0	76	12	10	0.5	0.4	0.1	
MD	2.1	17 ± 0.2	28 ± 0.2	35 ± 0.2	15 ± 0.2	3 ± 0.1	2 ± 0.1	27
REMD		17 ± 0.1	31 ± 0.2	33 ± 0.2	14 ± 0.1	3 ± 0.1	2 ± 0.0	
neutron diffraction	100.0	0.0	83.5	10.4	0.0	4.3	1.8	46

to a rather complex redistribution process between the different conformers. The most pronounced effect is the increase of the $\beta\gamma$ conformer probability with water concentration at the expense of the $\alpha\alpha$, $\alpha\beta$, and $\alpha\gamma$ fractions. Probably, the $\beta\gamma$ conformer, with its open geometry, is not capable of properly fitting into the hydrogen-bond network of pure glycerol, but it is able to form hydrogen bonds with water molecules instead.

3.2. Structure of Glycerol-Rich Glycerol−Water Mixtures. Radial distribution functions (RDF) contain the most basic information about the liquid structure. Several RDFs between different atom pairs are shown in Figure 6. Figure 6a contains the water oxygen−oxygen and oxygen−hydrogen RDFs. Adding glycerol in water strongly enhances the water structure and causes a noticeable increase in the intensity of water−water RDFs in the two first hydration layers. Comparison of water−water RDFs with the corresponding water−glycerol RDFs in Figure 6b shows that the height of the first peak of water−water RDFs is about 4 times higher than corresponding $O_{water}-O_{glycerol}$ and $O_{water}-H_{glycerol}$ RDFs. Both of these observations give a strong indication that, in the mixture, water molecules prefer to coordinate with other water molecules, forming water micro domains. Changes of glycerol−glycerol RDFs (between all oxygens in Figure 6c and between central carbons in Figure 6d) are not so dramatic. Still, one can see that at about 40 wt % of glycerol (system **I**), the $C_{central}-C_{central}$ glycerol RDF is higher than the corresponding RDF in pure liquid for all distances up to 8 Å. A similar effect, except a narrower region of the first RDF peak, is observed for oxygen−oxygen glycerol RDF. This gives an indication that even glycerol molecules in the mixture have a tendency to associate with each other. However, this trend is broken at the higher glycerol content (60 wt %, system **II**), which shows more uniform partitioning of glycerols among water molecules as compared to the case of 40 wt %.

A more detailed microscopic picture of the structure of glycerol−water mixtures can be obtained by using the spatial distribution functions (SDF) as iso-density maps of various atoms distributions relative to glycerol molecule. In the computation of iso-density SDFs, the space around a selected reference frame, fixed in the studied molecule(s), is divided into cubical segments with steps of 0.1 Å in all dimensions. The local density is then given as the average number of atoms in each segment divided by the segment volume and by the total average density. Three typical distributions for glycerol are shown in Figures 7−9. Figure 7 represents the distributions of glycerol oxygen and carbon atoms calculated in the reference frame formed by the three glycerol carbons, Figure 8 represents the distributions of water oxygens and hydrogens calculated in the same reference frame, and Figure 9 represents the SDFs of glycerol oxygen and carbon atoms as well as water oxygen and hydrogens around the terminal C−O−H molecular group of glycerol molecule.

Our results show that, within the studied glycerol concentrations, the shape of the SDFs does not change with increasing water content. Examination of the first solvation shell around glycerol for system **II** (100 glycerols per 340 water molecules) reveals that on average the three OH groups of a glycerol molecule are involved in approximately three hydrogen bonds, with glycerol and with water molecules, respectively, approximately 50−50%. At the half glycerol content, system **I** (50 glycerol molecules per 340 water), the share of water H-bond partners increases to approximately 55%. At the same time, the population of glycerol molecules in the first shell of water increases slightly, from 15% to 16%. Most probably, this H-bonding behavior can be explained from the fact that the glycerol H-bond network, typical for pure glycerol, still exists even at concentrations about 40 wt % of glycerol. This conclusion is in agreement with the observations based on the analysis of RDFs between all carbons where five pronounced maxima were observed in pure glycerol, four maxima were in 60.0 wt %, and three maxima (the fourth is very weak) were in 42.9 wt % solution, by contrast to Chen et al. data (see Figure 1A from ref 29), where a single weak maximum was observed in 29.7 wt % mixture. Possibly, while forming the first hydration shell around glycerol, water molecules

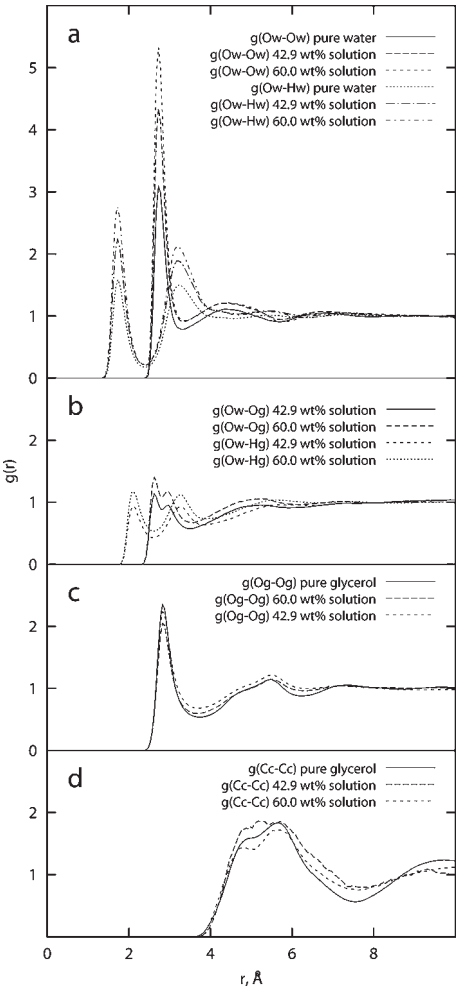

Figure 6. Radial distribution functions between different atom pairs: (a) $O_{water}-O_{water}$ and $O_{water}-H_{water}$; (b) $O_{water}-O_{glycerol}$ and $O_{water}-H_{glycerol}$; (c) $O_{glycerol}-O_{glycerol}$; and (d) $C_{central}-C_{central}$.

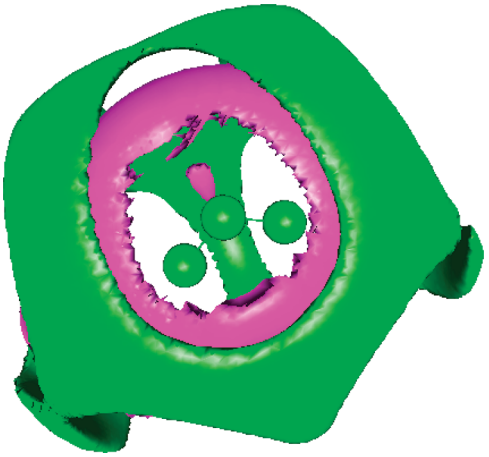

Figure 7. Spatial distributions of glycerol carbon (green) and glycerol oxygen (purple) around glycerol. System **III**. The density threshold is 2.5 times the bulk density.

slightly lose their ability to form hydrogen bonds. The average number of water molecule neighbors (calculated to the first

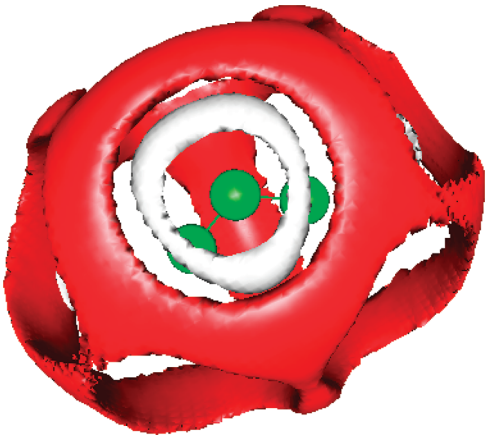

Figure 8. Spatial distributions of water oxygen (red) and hydrogen (white) around glycerol. System **II**. The density threshold is 2.5 times the bulk density.

Figure 9. Spatial distributions of water oxygen (red), water hydrogen (white), glycerol carbon (green), and glycerol oxygen (purple) around the terminal C−O−H molecular group of glycerol. System **I**. The density threshold is 2 times the bulk density.

minimum of oxygen−oxygen RDF) decreases from about 4.5 oxygens in pure SPC-F water to 3.9 (of which 0.6 with glycerol and 3.3 with water) for system **II**, and increases back to 4.4 (0.7 with glycerol and 3.7 with water) for system **I**. It means that at the studied concentrations water molecules tend to establish H-bonds much easier with themselves than with glycerol. This conclusion is consistent with the observations based on the analysis of RDF data (see above) and is in agreement with the results of neutron diffraction study by Malardier et al.[47] who found that water structure remains largely unpertubed in 5 water:1 glycerol mixture. This also explains the stability of glycerol H-bond network and agrees with the dielectric spectroscopy experimental data.[4,5]

3.3. Self-Association in Water−Glycerol Mixtures. Average atom distributions can not provide a full insight into the structure of glycerol−water solutions, which are quite heterogeneous systems. For water/organic-molecule solvent mixtures, hydrogen-bonding, hydrophobic, dipole−dipole interactions, etc., lead to the formation of microaggregates (clusters, domains) instead of free movement of the solvent.[48] According to the connectivity

Table 5. Probability Distributions of Molecules Connectivity in Water−Glycerol Mixtures in Percent

	water		glycerol	
molecule surrounding	system I	system II	system I	system II
$N_s = 0$	0.3	0.3	26.3	24.3
$0 < N_s < 0.5N_{pure}$	18.2	37.5	52.0	49.4
$0.5N_{pure} < N_s < N_{pure}$	32.0	37.1	10.2	16.0
$N_s \geq N_{pure}$	49.4	25.1	11.5	10.3

criterion of Stillinger,[49] two molecules are considered directly connected when their centers of mass (COM) are within a defined distance. In the present study, these distances were fixed to 3.35 Å around water and 7.5 Å around glycerol. These values are positions of the first minima of radial distribution functions of the COM of glycerol and water molecules in pure systems. In this way, the molecules in the mixtures can be classified into four groups: (i) isolated molecules (i.e., with no connectivity to any other molecule of the same type), (ii) molecules with the number of the neighbors of the same type (N_s) less than half of its value (N_{pure}) in the pure system, (iii) molecules with $0.5N_{pure} < N_s < N_{pure}$, and (iv) bulk-like molecules with $N_s \geq N_{pure}$. The calculated distributions are presented in Table 5. The local structure of water in 40−60 wt % mixtures is surprisingly close to its counterpart in pure water. The share of isolated water molecules is less than 1%. However, only 20−25% of glycerol molecules occur in surroundings similar to those in pure glycerol. About 25% of glycerols exist as monomers. Presumably, the structure of the remaining glycerols can be described as sequences of H-bonded strings connected with the remnants of the three-dimensional glycerol H-bond network in a "fluid" of water.

The time-averaged distributions of the sizes of the molecular aggregates in water−glycerol mixtures can be discussed in terms of either the number of the molecules involved or the size and shape of the cluster. In the present study, the concept of the cluster as a compact and roughly spherical droplet has been utilized. The size of microaggregate is defined as the number of the molecules of the same type inside the sphere, the radius of which is equal to the distance between the center of mass of chosen molecule and its closest neighbor of the other type. The sponge-like structures where each pair of particles is connected by an unbroken sequence (or chain) of molecules forming cavities, which incorporated a molecule of the other type, were not considered. The calculated distribution of cluster sizes (in percent) in glycerol−water mixtures is shown in Figure 10. At concentrations of about 40 wt %, the probabilities to find a water cluster of S particles are rather close for cluster sizes from 3 to 10 molecules. The increase of glycerol content leads to the depletion of clusters into the aggregates of smaller sizes. The water clusters of 3−5 molecules become the dominant structures. Nevertheless, the probability to find clusters consisting of 10 and more molecules still exists. These results are consistent with the neutron diffraction study of Towey et al.[50] who observed water aggregates of 7 molecules even in 1 water:4 glycerol mixture. For glycerol molecules, the size of microaggregates does not exceed 4 molecules, and most of the clusters are dimers. However, if the sponge-like structures with a single cavity are included in the consideration, the aggregates of up to 7 glycerol molecules are observed.

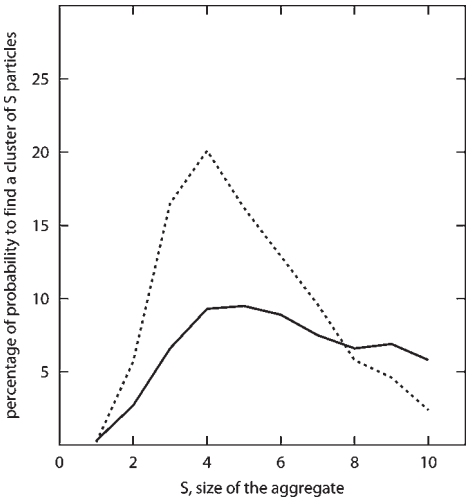

Figure 10. Probability distribution (in %) to find a water cluster of S particles. Solid line, data for system **I**; dotted line, for system **II**.

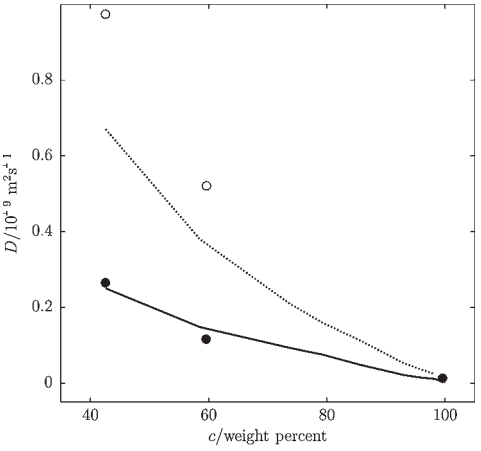

Figure 11. Concentration dependence of glycerol and water self-diffusion coefficients in glycerol−water mixtures at 25 °C and atmospheric pressure. Symbols "○" and "●" denote the result of simulation for water and glycerol respectively, the dotted line, experimental data for water; the solid line, for glycerol. The experimental data are taken from ref 51.

3.4. Self-Diffusion and Reorientational Motion. The water and glycerol self-diffusion coefficients computed from the mean square displacements of the molecules are given in Table 1 and shown in Figure 11 along with the experimental concentration dependences taken from ref 51. The simulation results for glycerol agree fairly well with the experimental data. For water molecules, the calculated self-diffusion coefficients are greater than the experimental ones. For pure water, the SPC-F model[35] also predicts somewhat faster diffusion, 2.47×10^9 m^2 s^{-1}, as compared to the experimental value of 2.30×10^9 m^2 s^{-1}.[52] However, in the case of the glycerol−water mixtures, the effect is more pronounced.

To investigate the molecular motion and rotational degrees of freedom in glycerol−water mixtures in more detail, the reorientational correlation functions, $C^\alpha = \langle P_1(\mathbf{e}^\alpha(t) \cdot \mathbf{e}^\alpha(0)) \rangle$, where P_1 is the first rank Legendre polynomial, and e^α is the unit vector pointed along the α axis in the molecular frame of each molecule,

were calculated. The corresponding correlation time, τ^{α}, can be estimated by fitting the correlation functions using the exponent: $C^{\alpha} = e^{-t/\tau\alpha}$. In the present analysis, three axes for water, the H−H vector, $\mathbf{R}_{HH}$, the molecular dipole, $\mathbf{R}_{D}$, and the normal to the plane of the molecule, $\mathbf{R}_{P}$, and the molecular dipole vector for glycerol were considered. The spatial distribution functions (see Figure 8) demonstrated that water orientation in the vicinity of an OH group of glycerol molecule can be described as so-called H-bonded configuration, when one of the water hydrogens is located on the radial vector $O_{glycerol}-O_{water}$, whereas the second water hydrogen points away. The symmetric configuration of water (where the water hydrogen arrangement is symmetric with respect to the radial vector) was not observed in the present simulations. The reorientational correlation times were calculated for all water molecules as well as for selected substructures, for example, for water molecules in the glycerol first solvation shell. The results are collected in Table 6.

Despite many experimental studies on pure glycerol and glycerol−water mixtures,[4,5,53−59] dynamical behavior of neither glycerol nor water is not yet completely understood. According to experimental estimations, typical correlation times for glycerol motion are of the order of $10^{-9}-10^{-10}$ s. However, the measured quantities are usually interpreted in terms of correlation times, which are associated with a specific type of molecular motion. The validity of such assumptions does not rest on any solid physical basis, especially in the case of glycerol, which is capable of forming both intramolecular and intermolecular hydrogen bonds and most likely undergoes even conformational changes during the reorientations. The unambiguous interpretation of experimental data still remains problematic.

The present simulations indicate that, as it could be expected, the presence of water allows a higher glycerol mobility, the glycerol slows the water mobility, and the effect becomes more pronounced with increasing the glycerol content. The calculated glycerol reorientational times are of the order of tens of picoseconds. According to MD simulations of Chelli et al.,[19] the average lifetime for a backbone conformation in pure glycerol is about 200−250 ps for pure glycerol at 300 K. The reorientational correlation times obtained cannot be associated with the conformational jumps. Considering the dynamical properties of the hydrogen-bond network in pure glycerol, Chelli and coauthors[19] observed that the breakdown of H-bond network occurs due to three mechanisms: the vibrational motion of a glycerol molecule in the cage formed by its neighbors, the exchange of the neighbors forming the cage, and the translational diffusion. The characteristic correlation time for the second mechanism is equal to 18.3 ps at 320 K.[19] This value is rather close to the data reported in Table 6. Most likely, the reorientations of glycerol molecules in glycerol−water mixtures are controlled by the exchange of the neighbors involved in H-bonds.

For waters, not hydrogen bonded to glycerol, the reorientational correlation time of the dipole moment corresponds to the slowest motion. The dynamics of water molecules involved in forming the first solvation shell around glycerol changes completely. First, the correlation times are much longer. Second, despite the rather fast exchange with the rest of water molecules (the average lifetime is about 4−5 ps), the reorientation of $\mathbf{R}_{HH}$ vector becomes the slowest motion. The simulations of concentrated mixtures also show that the central and terminal OH groups of glycerol are nonequivalent in considering water H-bond dynamics. For system **I**, the reorientational correlation times for water molecules involved in hydrogen bonding with

Table 6. Reorientational-Rotational Correlation Times for Water and Glycerol Molecules in Various Systems and Solution Substructures

			vector		
			$\mathbf{R}_{HH}$	$\mathbf{R}_{D}$	$\mathbf{R}_{P}$
system	molecule	substructure	τ, ps	τ, ps	τ, ps
IV	water		4.48 ± 0.04	5.39 ± 0.11	3.27 ± 0.06
III	glycerol			39 ± 2	
II	water	H-bonded to $O_{terminal}$	63 ± 7	52 ± 9	38 ± 6
II	water	H-bonded to $O_{central}$	48 ± 3	39 ± 4	29 ± 3
II	water	whole water	13 ± 1	16 ± 1	10 ± 1
II	glycerol			15.8 ± 0.6	
I	water	H-bonded to $O_{terminal}$	27 ± 5	19 ± 3	14 ± 2
I	water	H-bonded to $O_{central}$	27 ± 3	19 ± 2	14 ± 2
I	water	whole water	8 ± 1	10 ± 1	6 ± 1
I	glycerol			10.9 ± 0.4	
			τ:$\tau_{pure\ water}$	τ:$\tau_{pure\ water}$	τ:$\tau_{pure\ water}$
IV	water		1:1	1:1	1:1
II	water	H-bonded to $O_{terminal}$	14.1:1	9.6:1	11.6:1
II	water	H-bonded to $O_{central}$	10.7:1	7.2:1	8.9:1
II	water	whole water	2.9:1	3.0:1	3.1:1
I	water	H-bonded to $O_{terminal}$	6.0:1	3.5:1	4.3:1
I	water	H-bonded to $O_{central}$	6.0:1	3.5: 1	4.3:1
I	water	whole water	1.8:1	1.9:1	1.8:1

central and terminal OH groups of glycerol are practically the same. With increasing of the glycerol concentration, the mobility of water in the vicinity of the central group becomes 1.3 times faster as compared to those close to the terminal groups. This result indicates that the hydrogen bonds involving the central OH group are weaker, allowing the higher water mobility.

4. CONCLUSIONS

In our work, structural and dynamical properties of concentrated glycerol−water mixtures have been studied by classical MD simulations. Two glycerol−water mixtures, 42.9 and 60.0 wt % of glycerol, as well as pure glycerol were simulated to investigate systematically the effect of water.

All-atom conformational distributions for glycerol have been analyzed in terms of Ramachandran plots, indicating the permitted values of neighboring torsion angles. The $\alpha\alpha$ backbone conformer is found to be the most abundant for all studied glycerol−water mixtures. The $\beta\beta$ and $\gamma\gamma$ conformers give only a negligible contribution. All other forms, $\alpha\beta$, $\alpha\gamma$, and $\beta\gamma$, contribute about 60% in total. It was found that the presence of water molecules causes a rather complex redistribution process between various conformers. The main effect is the increase of the $\beta\gamma$ conformer probability with water concentration at the expense of the $\alpha\alpha$, $\alpha\beta$, and $\alpha\gamma$ fractions.

The local structure of water in 40−60 wt % mixtures is surprisingly close to its counterpart in pure water. The share of

isolated water molecules is less than 1%. On the other hand, only 20−25% of glycerol molecules occur in surrounding similar to pure system. About 25% of glycerol molecules exist as monomers. Presumably, the structure of the rest of glycerols can be described as the set of H-bonded strings connected with the remnants of the three-dimensional glycerol H-bond network in a "fluid" of water. Nevertheless, the glycerol H-bond network typical for pure glycerol still exists even at concentrations of about 40 wt % of glycerol.

The heterogeneity of water−glycerol mixtures can be described in terms of the time-averaged distributions of the sizes of the water aggregates. In the present study, the size of microaggregate was defined as a number of the water molecules inside the sphere whose radius is equal to the distance between centers of mass of chosen water molecule and the closest glycerol. At concentrations of about 40 wt %, the probabilities of finding a water cluster of S particles are rather close for cluster sizes from 3 to 10 molecules. The increase of glycerol content leads to the depletion of clusters into the aggregates of smaller sizes. The water clusters of 3−5 molecules become the dominant structures.

The calculated reorientational correlation functions and corresponding correlation times for water and glycerol molecules clearly indicate that the presence of water increases the glycerol mobility. In its turn, the glycerol slows the water reorientations. The corresponding reorientational correlation times are of the order of tens of picoseconds. Most likely, the glycerol reorientations can be associated with the H-bond neighbors exchange rather than with the conformational jumps. The dynamics of water molecules forming the glycerol first solvation shell changes completely despite the rather fast exchange with the rest of water. The simulation results also show that in concentrated mixtures, the water's hydrogen-bonding dynamics is different when close to the central and terminal OH groups of glycerol.

AUTHOR INFORMATION

Corresponding Author

*E-mail: aatto@mmk.su.se.

ACKNOWLEDGMENT

We thank Dr. Cong Chen (Dalian University of Technology, China) for his valuable help and Dr. Francesca Mocci for valuable comments. The financial support by the grants of The Human Capital Foundation (Russia), The Russian Foundation for Basic Research (grant 10-03-01043a), and The Swedish Science Council (VR) are gratefully acknowledged. The Swedish National Infrastructure in Computing (SNIC) is acknowledged for the computing grant.

REFERENCES

(1) Cicerone, M. T.; Soles, C. L. *Biophys. J.* **2004**, *86*, 3836.
(2) Ueda, M.; Katayama, A.; Kuroki, N.; Urabata, T. *Colloid Polym. Sci.* **1976**, *254*, 532.
(3) Baldelli, S.; Schnitzer, C.; Schultz, M. J.; Campbell, D. J. *J. Phys. Chem. B* **1997**, *101*, 4607.
(4) Puzenko, A.; Hayashi, Y.; Ryabov, Y. E.; Balin, I.; Feldman, Y.; Kaatze, U.; Behrends, R. *J. Phys. Chem. B* **2005**, *109*, 6031.
(5) Hayashi, Y.; Puzenko, A.; Feldman, Y. *J. Non-Cryst. Solids* **2006**, *352*, 4696.
(6) Shulgin, I. L.; Ruckenstein, E. *J. Chem. Phys.* **2005**, *123*, 054909.
(7) Sedgwick, H.; Cameron, J. E.; Poon, W. C. K.; Egelhaaf, S. U. *J. Chem. Phys.* **2007**, *127*, 125102.
(8) Rariy, R. V.; Klibanov, A. M. *Proc. Natl. Acad. Sci. U.S.A.* **1997**, *94*, 13520.
(9) Chen, B.; Sigmund, E. E.; Halperin, W. P. *Phys. Rev. Lett.* **2006**, *96*, 145502.
(10) Root, L. J.; Stillinger, F. H. *J. Chem. Phys.* **1989**, *90*, 1200.
(11) Root, L. J.; Stillinger, F. H. *Phys. Rev. B* **1990**, *41*, 2348.
(12) Root, L. J.; Berne, B. J. *J. Chem. Phys.* **1997**, *107*, 4350.
(13) Benjamin, I.; Wilson, M.; Pohorille, A. *J. Chem. Phys.* **1994**, *100*, 6500.
(14) Benjamin, I.; Wilson, M.; Pohorille, A.; Nathanson, G. M. *Chem. Phys. Lett.* **1995**, *243*, 222.
(15) Padro, J. A.; Saiz, L.; Guardia, E. *J. Mol. Struct.* **1997**, *416*, 243.
(16) Guardia, E.; Marti, J.; Padro, J. A.; Saiz, L.; Komolkin, A. V. *J. Mol. Liq.* **2002**, *96−97*, 3.
(17) Jorgensen, W. L. *J. Phys. Chem.* **1986**, *90*, 1276.
(18) Chelli, R.; Procacci, P.; Cardini, G.; Della Valle, R. G.; Califano, S. *Phys. Chem. Chem. Phys.* **1999**, *1*, 871.
(19) Chelli, R.; Procacci, P.; Cardini, G.; Califano, S. *Phys. Chem. Chem. Phys.* **1999**, *1*, 879.
(20) Chelli, R.; Gervasio, F. L.; Gellini, C.; Procacci, P.; Cardini, G.; Schettino, V. *J. Phys. Chem. A* **2000**, *104*, 11220.
(21) Racko, D.; Chelli, R.; Cardini, G.; Bartos, J.; Califano, S. *Eur. Phys. J. D* **2005**, *32*, 289.
(22) Blieck, J.; Affouard, F.; Bordat, P.; Lerbret, A.; Descamps, M. *Chem. Phys.* **2005**, *317*, 253.
(23) Callam, C. S.; Singer, S. J.; Lowary, T. L.; Hadad, C. M. *J. Am. Chem. Soc.* **2001**, *123*, 11743.
(24) Zhuang, W.; Dellago, C. *J. Phys. Chem. B* **2004**, *108*, 19647.
(25) Dashnau, J. L.; Nucci, N. V.; Sharp, K. A.; Vanderkooi, J. M. *J. Phys. Chem. B* **2006**, *110*, 13670.
(26) Reiling, S.; Schlenkrich, V.; Brickmann, J. *J. Comput. Chem.* **1996**, *17*, 450.
(27) Yongye, A. B.; Foley, B. L.; Woods, R. J. *J. Phys. Chem. A* **2008**, *112*, 2634.
(28) Chen, C.; Li, W. Z.; Song, Y. S.; Yang, J. *J. Mol. Liq.* **2009**, *146*, 23.
(29) Chen, C.; Li, W.-Z. *Acta Phys.-Chim. Sin.* **2009**, *25*, 507.
(30) Kyrychenko, A.; Dyubko, T. S. *Biophys. Chem.* **2008**, *136*, 23.
(31) Busselez, R.; Lefort, R.; Ji, Q.; Affouard, F.; Morineau, D. *Phys. Chem. Chem. Phys.* **2009**, *11*, 11127.
(32) *CRC Handbook of Chemistry and Physics*; CRC Press: Boca Raton, FL, London, New York, Washington, DC, 2000.
(33) Hatcher, E. R.; Guvench, O.; MacKerell, A. D. *J. Chem. Theory Comput.* **2009**, *5*, 1315.
(34) Melberg, S.; Rasmussen, K. *J. Mol. Struct.* **1979**, *57*, 215.
(35) Toukan, A. K.; Rahman, A. *Phys. Rev. B* **1985**, *31*, 2643.
(36) Guillot, B. *J. Mol. Liq.* **2002**, *101*, 219.
(37) Lyubartsev, A. P.; Laaksonen, A. *Comput. Phys. Commun.* **2000**, *128*, 565.
(38) Nosé, S. *Mol. Phys.* **1984**, *52*, 255.
(39) Martyna, G. J.; Tobias, D. J.; Klein, M. L. *J. Chem. Phys.* **1994**, *101*, 4177.
(40) Martyna, G. J.; Tuckerman, M. E.; Tobias, D. J.; Klein, M. L. *Mol. Phys.* **1996**, *87*, 1117.
(41) Tuckerman, M.; Berne, B. J.; Martyna, G. J. *J. Chem. Phys.* **1992**, *97*, 1990.
(42) Bastiansen, O. *Acta Chem. Scand.* **1949**, *3*, 415.
(43) Ramachandran, G. N.; Sasisekharan, V. *Adv. Protein Chem.* **1968**, *23*, 283.
(44) Ramachandran, G. N.; Mitra, A. K. *J. Mol. Biol.* **1976**, *107*, 85.
(45) van Koningsveld, H. *Recl. Trav. Chim. Pays-Bas* **1970**, *89*, 801.
(46) Towey, J. J.; Soper, A. K.; Dougan, L. *Phys. Chem. Chem. Phys.* **2011**, *13*, 9397.
(47) Malardier-Jugroot, C.; Bowron, D. T.; Soper, A. K.; Johnson, M. E.; Head-Gordon, T. *Phys. Chem. Chem. Phys.* **2010**, *12*, 382.

(48) Dixit, S.; Crain, J.; Poon, W. C. K.; Finney, J. L.; Soper, A. K. *Nature* **2002**, *416*, 829.
(49) Stillinger, F. H. *J. Chem. Phys.* **1963**, *38*, 1486.
(50) Towey, J. J.; Soper, A. K.; Dougan, L. *J. Phys. Chem. B* **2011**, *115*, 7799.
(51) D'Errico, G.; Ortona, O.; Capuano, F.; Vitagliano, V. *J. Chem. Eng. Data* **2004**, *49*, 1665.
(52) Weingärtner, H. *Z. Phys. Chem. N. F.* **1982**, *132*, 129.
(53) Noack, F.; Preissing, G. *Z. Naturforsch., A* **1969**, *24*, 143.
(54) Drake, P. W.; Meister, R. *J. Chem. Phys.* **1971**, *54*, 3046.
(55) Fiorito, R. B.; Meister, R. *J. Chem. Phys.* **1972**, *56*, 4605.
(56) Kintzinger, J. P.; Zeidler, M. D. *Ber. Bunsen-Ges.* **1973**, *77*, 98.
(57) Burnett, L. J.; Roeder, S. B. W. *J. Chem. Phys.* **1974**, *60*, 2420.
(58) Wolfe, M.; Jonas, J. *J. Chem. Phys.* **1979**, *71*, 3252.
(59) Friedrich, A.; Dölle, A.; Zeidler, M. D. *Magn. Reson. Chem.* **2003**, *41*, 813.